2016 IEEE Conference on Control Applications (CCA)
Part of 2016 IEEE Multi-Conference on Systems and Control
September 19-22, 2016. Buenos Aires, Argentina

Integral Terminal Sliding Mode Control for Maximum Power Production in Grid Connected PV Systems

Sai Sree Teja Amirineni, Mohammad Javad Morshed, and Afef Fekih, Senior Member, IEEE

Abstract—**Photovoltaic (PV) systems have gained an ever increasing popularity as a renewable energy source. However, designing control schemes that ensure maximum power extraction for grid-connected PV arrays while properly mitigating grid faults is still a challenging problem in the control community. This paper proposes an integral terminal sliding mode control (ITSM) scheme for grid-connected PV arrays. The approach aims at maximizing power extraction while mitigating the effects of disturbances caused by irradiance fluctuations and oscillations in the bulk voltage. Effective elimination of the voltage drag and maximum power point tracking are among the positive features of the proposed approach. Efficiency of the proposed approach was assessed using a simulation study involving several operating conditions and various faulty situations.**

Index Terms— **Photovoltaic, Integral terminal sliding mode control, electric power quality.**

NOMENCLATURE

PV	Photovoltaic.
P & O	Perturb and observe.
MPPT	Maximum power point tracking.
MPP	Maximum power point
SMC	Sliding mode control.
TSMC	Terminal sliding mode control.
IGBT	Insulated gate bipolar transistors.
SPDT	Single pole double throw.
MOSFET	Metal oxide semiconductor field effect transistor.
BJT	Bipolar junction transistor.
I_{SC}	Current generated by incident light (or) Short circuit current.
I_o	Reverse saturation current.
q	Electron charge is equal to $1.602 \times 10^{-19} C$.
K	Boltzmann constant is equal to $1.38 \times 10^{-23} J/K$.
T	Temperature of p-n junction in kelvin.
A	Ideal diode constant.
I_{or}	Nominal saturation current.
T_R	Nominal temperature.
E_g	Band gap energy of the semiconductor.
V_{OC}	Open circuit voltage.

This work is partially supported by the Louisiana Board of Regents Support Fund contract number LEQSF-EPS (2015)-PFUND-421 and LEQSF (2012-15)-RD-A-26.

S.T.Amirineni, M.J. Morshed and A. Fekih are with the Department of Electrical and Computer Engineering at the University of Louisiana at Lafayette, Lafayette, LA 70504, USA (e-mails: sxa7892@louisiana; morshed@louisiana.edu; afef.fekih@louisiana.edu).

I. INTRODUCTION

Thanks to their their affordable cost and simple design, photovoltaic (PV) systems are gaining popularity as a clean energy source [1]-[2]. A PV structure is typically comprised of a PV array, a DC/DC converter and an inverter. PV characteristics and power production capabilities depend on various factors such as irradiance level, shades, temperature, among others. The operation point at which maximum power is attained is called maximum power point (MPP). This operating point is greatly influenced by environmental parameters which makes designing controllers for maximum power point tracking (MPPT) quite challenging.

Among the control approaches proposed for MPPT [3], PI-based controllers are the most popular [4]. However, it is well known that PI controllers are not robust against parametric uncertainties, external disturbances and un-modeled dynamics. Fuzzy controllers were also considered in designing PV control systems [5][6]. However, fuzzy systems are very restricted since they abide to their pre-defined rules. Also they are not robust against the topological changes of the system. Adaptive controllers have also been considered in the control of PV power systems [7][8]. Hence, advanced control designs should be considered to provide high accuracy in MPP tracking and fast convergence rate regardless of the load and environmental conditions.

Sliding Mode Control (SMC) is a powerful approach when the control objective is to provide robustness to uncertainties and external disturbances [9]-[10]. This nonlinear control strategy can withstand input constraint deviations and also provides fast moving feedback [11]. It operates by driving the nonlinear path to a predefined surface while upholding the state trajectory on this surface every time [12]. Some sliding mode-based control approaches have been proposed to mitigate load voltage oscillations and accurately track the reference provided by the MPPT algorithm [13]. However, these approaches cannot guarantee the existence of the sliding mode for the entire operating range. Since linear sliding surface of a standard SMC exhibits asymptotic steadiness, higher order terms such as TSMC were proposed [14]. TSMC attains finite-time convergence and ensures high precision and accuracy when following a given command. However, the use of fractional power functions as the sliding hyperplane in TSM design leads to intrinsic singular problems. Hence, TSM performance can further be improved by introducing an integral term leading to

ITSMC designs. This will effectively eliminate supplementary steady state error glitches. Further ITSMCs lead to a less pronounced chattering effect compared to the standard SMC [19].

This paper proposes a novel ITSMC control scheme for grid-connected PV arrays subject to uncertainties and irradiant fluctuations. The main contributions of this paper are as follows:

- Design of a new integral terminal sliding mode control (ITSMC) for a grid-connected PV systems.
- Implementation of a new ITSMC-based MPPT scheme for stand-alone PV power systems.

The rest of the paper is organized as follows. The grid-connected PV power generation system is discussed in section II. Section III provides the necessary details for the design of the proposed ITSMC approach for the grid connected PV. Computer experiments are provided in sections IV to demonstrate the effectiveness of the proposed control strategy in achieving maximum power under various disturbances. Finally, concluding remarks are drawn in section V.

II. System Structure

A. PV cell modelling

A PV cell is made up of a semiconductor diode. Once the photon of light strikes the PV cell, the outer electron breaks the bond in the semiconductor device, and electrons are emitted when the energy of the photon is greater than the band gap energy. Thus, a semiconductor device that converts light into electrical energy by the photovoltaic effect is recognized as the photovoltaic cell or photoelectric cell [20]. The overall phenomenon is termed as the absorption of solar rays, ejection of electrons and collection of these free charges at the end of the PV system.

Consider the Shockley diode equation of a single diode PV cell [21]:

$$I_D = I_o \left[exp\left(\frac{qV_{PV}}{AKT}\right) - 1 \right] \quad (1)$$

The output PV current with output PV voltage V_{PV} is defined by:

$$I_{PV} = I_{SC} - I_o \left[exp\left(\frac{qV_{PV}}{AKT}\right) - 1 \right] \quad (2)$$

where the variation of the reverse saturation current I_o of a PV cell is given by:

$$I_o = I_{or} \left[\frac{T}{T_R}\right]^3 \exp\left(\frac{qE_g}{K\alpha}\left[\frac{1}{T_R} - \frac{1}{T}\right]\right) \quad (3)$$

where the considered parameters are described in the nomenclature.

B. Grid-connected PV array

The schematic diagram of a grid connected PV array is depicted in Fig. 1. Note that the PV array is linked to the DC-DC converter and then to the DC-AC inverter, which is in tern connected to the grid. Here I_{PV} and V_{PV} are gauged from the PV array and are fed to the perturb and observe algorithm [22], which generates the reference voltage at the maximum power. The reference voltage is then delivered to the ITSMC controller whose objective is to keep the output voltage in track with the reference voltage. This is achieved by controlling and modifying the duty cycle. The resulting duty cycle is given to the PWM generator which produce the PWM signals for the IGBT of the DC-DC converter.

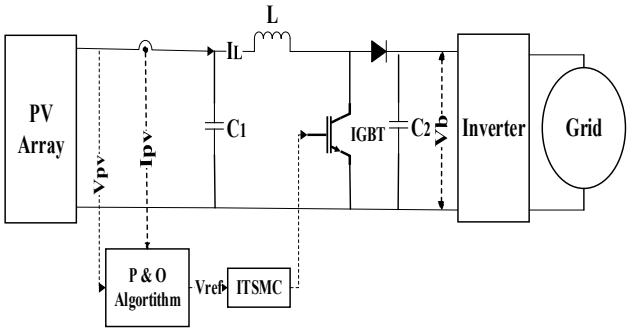

Fig. 1. Topology of a grid-connected PV array

A fundamental DC-DC converter circuit also known as boost converter is illustrated in Fig.1. A single-pole double-throw (SPDT) switch is connected to the DC input voltage as shown. SPDT switches are semiconductor devices, such as diodes, power MOSFETs, IGBTs, BJTs, or thyristors [23]. IGBT provides better power gain than the usual bipolar type transistors, since they combine the higher voltage operation of the bipolar type transistor and lower input losses of MOSFET [24]. Hence, IGBTs (Insulated Gate Bipolar Transistors) are often favored over BJT or MOSFET.

A DC-DC boost converter is connected to regulate the output voltage of the PV array (V_{PV}) and achieve maximum solar power generation. The capacitor current is given by [17]:

$$I_{C_1} = C_1 \frac{dV_{PV}}{dt} = I_{PV} - I_L, \quad (4)$$

where I_L is the inductor current.
The voltage across the inductor L is given by:

$$V_L = L \frac{dI_L}{dt} = V_{PV} - V_b(1-u), \quad (5)$$

where u is the duty cycle given to the IGBT switch and V_b is the bulk voltage across the capacitor C_2.

C. MPP searching

Before MPP, the key characteristics of a PV cell are the short circuit current and open circuit voltage. The current that we get from the PV cell at zero load resistance is

described as the short circuit current. The current is zero and the open circuit voltage is maximum when the load resistance is the infinity. In both cases the obtained power is zero. Maximum power is obtained when the combination of best voltage and current is achieved as illustrated in Fig. 2.

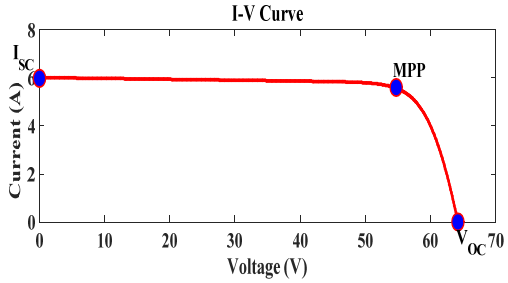

Fig. 2. I-V characteristic curve showing important points

To enhance the efficiency of the solar device, a maximum power point tracking algorithm is essential. There are numerous methods for MPPT, such as perturb and observe, incremental conductance, fractional short circuit current, fractional open circuit voltage, fuzzy control, neural network control, etc. [25]. Though there are many advancements in tracking maximum power we choose perturb and observe algorithm for its simplicity and popularity for less implementation cost. Perturb and observe technique has quite a few benefits, such as its simple implementation, optimum MPP tracking time and reasonable cost effectiveness [13].

Fig. 3 shows general flowchart for the perturb and observe algorithm, which tracks the maximum power point by changing the PV voltage in accordance with the reference voltage generated by the algorithm.

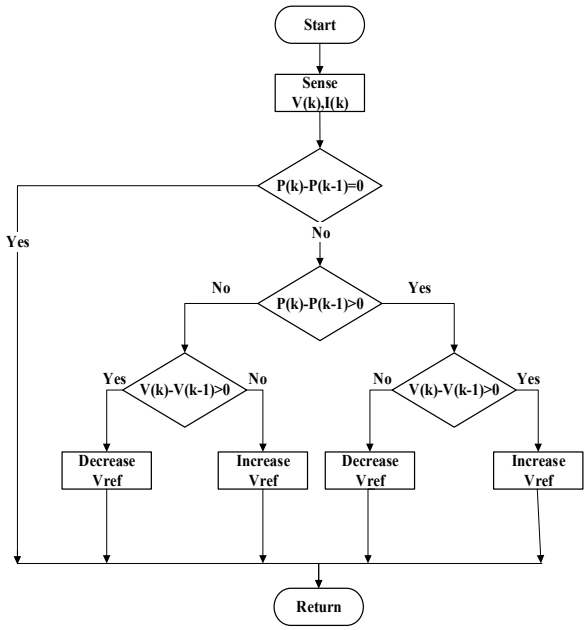

Fig. 3. MPPT flowchart of proposed approach

The change in the PV voltage depends on the PV power. Hence, the reference voltage is altered accordingly. For instance, during a rise in power, the perturbation should be in the same direction. When, power in being reduced, the perturbation will continued in the opposite direction. The whole phenomenon repeats until the MPP is attained.

III. Control Scheme

Due to the unhinged instantaneous dc input and ac output powers, voltage ripples often occur on the dc link voltage at the output of the boost converter in grid-connected PV systems. This ripple leads to fluctuations in the PV output voltage, as well as sudden variations in the input voltage of the boost converter [26]. This will lead to power losses due to the resulting improper MPP operations. Hence, the proposed approach ITSMC is designed for the proper MPPT control under uncertain conditions. The aim of the ITSMC is to hold the system error on an integral terminal sliding surface and then unite this error to the origin in finite time [27].

Consider the following switching variable for a grid-connected PV device:

$$s = e(t) + \alpha e_i(t), \tag{6}$$

where $e(t) = V_{PV} - V_{ref}$ refers to the error between the output PV voltage V_{PV} and the reference voltage V_{ref} and $e_i(t)$ is the integral term added to the original error $(\ddot{e}_i(t) = sign(e(t)))$. Also, α is a constant coefficient which is greater than zero.

Consider the following sliding manifold σ:

$$\sigma = \dot{e}(t) + \alpha \dot{e}_i(t) \tag{7}$$

The control signal is obtained when $\dot{\sigma} = 0$. Thus,

$$\dot{\sigma} = \ddot{e}(t) + \alpha \ddot{e}_i(t) = 0 \tag{8}$$

Equation (8) leads to:

$$\dddot{V}_{PV} - \dddot{V}_{ref} + \alpha \ddot{e}_i(t) = 0 \tag{9}$$

Equation (4) provides the expression of $\dddot{V}_{PV}$, which when substituted to (9) leads to,

$$\frac{1}{C_1}\left[\ddot{I}_{PV} - \ddot{I}_L\right] - \dddot{V}_{ref} + \alpha \ddot{e}_i(t) = 0 \tag{10}$$

Substituting (5) in (10) yields:

$$u = \frac{1}{V_b}\left[L\ddot{I}_{PV} + LC_1\alpha \ddot{e}_i(t) - LC_1\dddot{V}_{ref} - V_{PV} + V_b - ksign(s)\right] \tag{11}$$

where k is a positive constant. Note that $\dddot{V}_{ref}$ is bounded and is within acceptable ranges thus achieving proper performance of the proposed approach.

Proof:

Consider the following Lyapunov function:

$$V = \frac{1}{2}\sigma^2 \tag{12}$$

Here we need to prove that the derivative of V is negative in order to assure the convergence of V

$$\dot{V} = \sigma\dot{\sigma} < 0 \tag{13}$$

Substituting equation (8) in equation (13) we get

$$\dot{V} = \sigma\{\ddot{e}(t) + \alpha\ddot{e}_i(t)\} \tag{14}$$

$$\dot{V} = \sigma\left\{\frac{1}{C_1}\left[\dot{I}_{PV} - \dot{I}_L\right] - \ddot{V}_{ref} + \alpha\ddot{e}_i(t)\right\}$$

$$= \sigma\left\{\frac{1}{C_1}\dot{I}_{PV} - \frac{1}{LC_1}V_{PV} + \frac{1}{LC_1}V_b(1-u) - \ddot{V}_{ref} + \alpha\ddot{e}_i(t)\right\}$$

$$= ||\sigma||\left\{||\frac{\dot{I}_{PV}}{C_1}|| - ||\frac{V_{PV}}{LC_1}|| + ||\frac{V_b}{LC_1}|| - ||\frac{V_b}{LC_1}||u - ||\ddot{V}_{ref}|| + \alpha||\ddot{e}_i(t)||\right\} \tag{15}$$

Substituting *u* in the above equation yields:

$$\dot{V} \le ||\sigma||\left\{-||\frac{V_b}{LC_1}||k\right\}$$

$$\dot{V} \le -||\sigma||\left\{||\frac{V_b}{LC_1}||k\right\} \tag{16}$$

It is obvious that if (16) holds then the exponential convergence of *e* to zero is guaranteed.

IV. COMPUTER EXPERIMENTS

To assess the performance of the proposed control scheme, we performed a series of computer simulations under various operating conditions. The solar panel considered in the simulation is the *SunPower SPR-305E-WHT-D* with 96 cells per module. The array consists of 66 parallel strings and 5 series connected modules per string. The capacitor C_1 value is considered as 100 μF, and the inductor L is chosen with a value of 5 mH. A diode with 0.1 $m\Omega$ is connected to capacitor C_2, which is given as 24 mF. In ITSMC k is chosen to be 5 and α is 0.5. The switching frequency of the voltage source converter is 60 Hz, and for the PWM it is 5000. The initial value of the duty cycle is considered as 0.5. Ideally the PV array can deliver a maximum of 100 W/m^2 at 1000 W/m^2 irradiance with a total of 330 sun power modules.

The following scenarios illustrating the controller performance under varying irradiance conditions were considered:

A. Scenario-1

Consider the irradiance as 1000 W/m^2 at 25°C. Fig. 5 shows the output power from the transformer, which is fed into the utility grid. Fig. 4 shows the output voltage of boost converter.

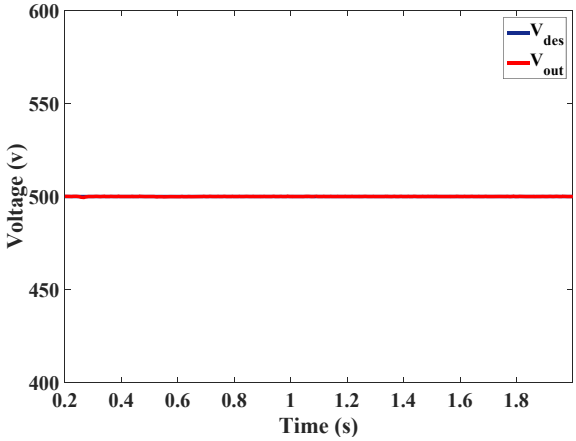

Fig. 4. Output voltage of boost converter for scenario-1

In Fig. 4 the V_{des} is the desired output voltage and V_{out} is the output voltage. The desired output voltage is chosen as 500. While coming to Fig. 5, we can observe that the maximum power is achieved.

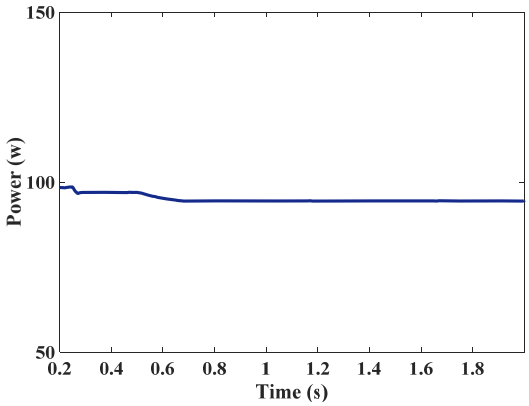

Fig. 5. Power fed into the grid for scenario-1

B. Scenario-2

Now let us consider the irradiance, which is changing. This change is shown in Fig. 6. Then the output power of the transformer and the output voltage of the boost converter are varied and are shown in Fig. 7 and Fig. 8, respectively.

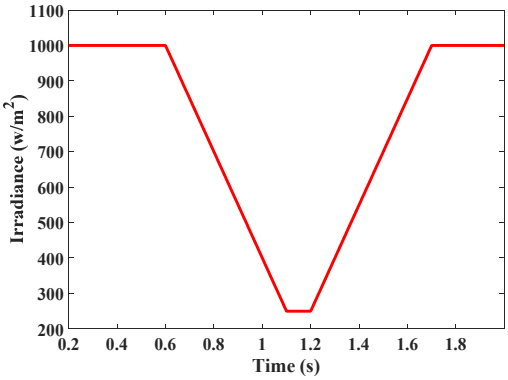

Fig. 6. Irradiance given to PV module in scenario-2 and scenario-3

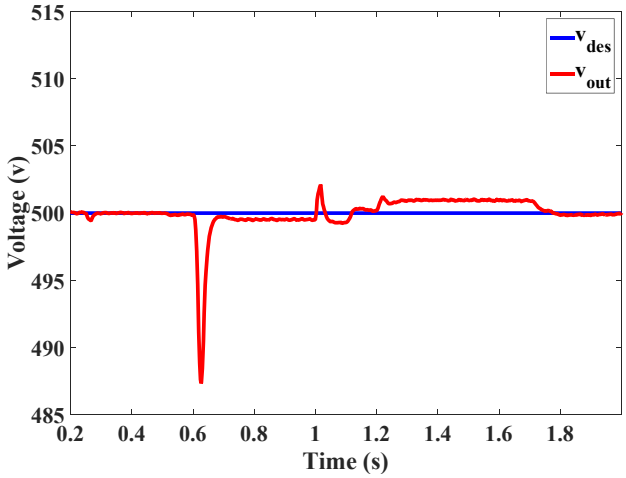

Fig. 7. Output voltage of boost converter for scenario-2

Here we can observe that there is a change in irradiance from 0.6 sec, and though the voltage curve has a bump, it is settling soon and is on track again. Thus, from Fig. 7 it is clear that, despite the change in irradiance, the controller was able to maintain the voltage close to its desired value. We can also observe the absence of the chattering effect while tracking for maximum power.

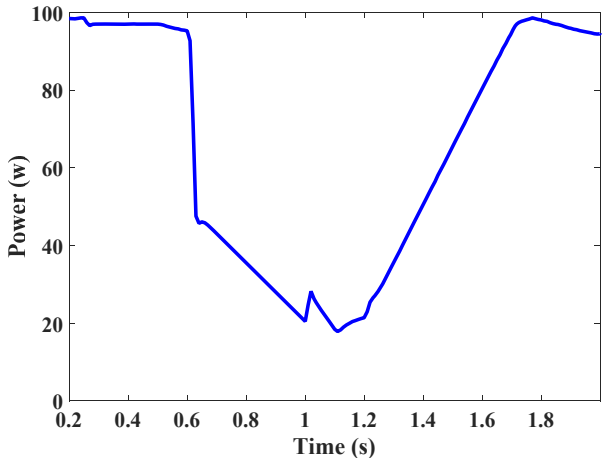

Fig. 8. Power fed into the grid for scenario-2

Fig. 8 shows the output power, which varies along with the irradiance, as depicted in Fig. 6. Here also, we notice the chattering-free performance despite the continuous change in irradiance.

C. Scenario-3

A fault can occur unexpectedly in the system. Consider an abrupt fault stimulated by a step function at 0.5 sec. Now, let's consider a temperature of 25 ^{o}C and the irradiance depicted in Fig. 6 as our inputs. The resulting output voltage of the boost converter is depicted in Fig. 9.

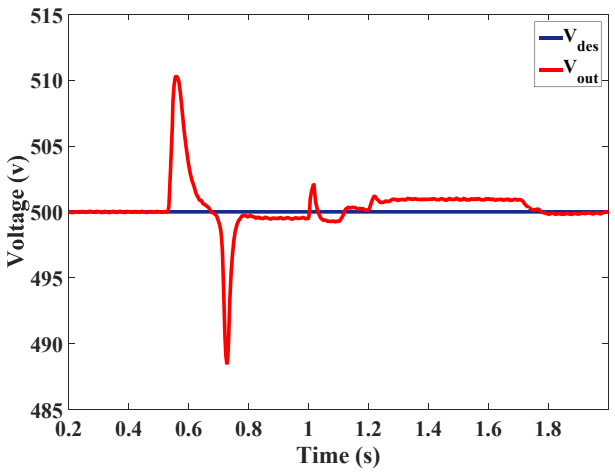

Fig. 9. Output voltage of boost converter for scenario-3

Note from Fig. 9 that though a deviation in irradiance triggers a voltage sag, this latter subsides fairly quickly. The system's response is reasonable with a settling time around 1.2 sec. Hence, despite the idisturbances, the ITSMC was able to effectively control the PV array and properly track the reference in reasonable time. This further confirms the controller's robustness. Note also, that despite the unfavorable conditions, the ITSMC was able to track the maximum power as shown below.

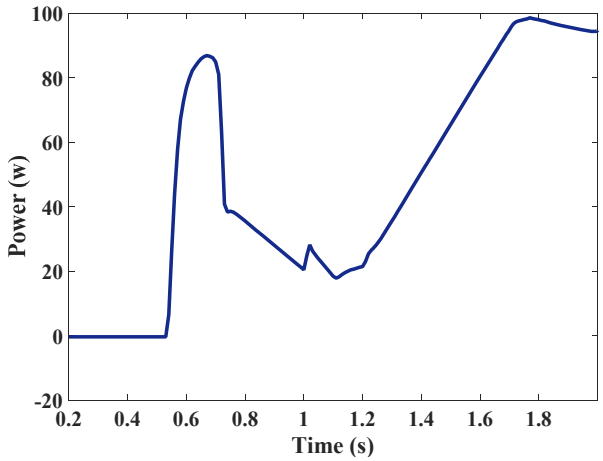

Fig. 10. Power fed into the grid for scenario-3

Fig. 10 depicts the variations of the output power. This latter is shown to exhibit a chattering-free performance.

From the above scenarios, we can conclude that the ITSMC can properly mitigate deep voltage sags caused by input variations and external disturbances. Scenario-1 shows the power generated by the grid-connected PV module. Under these conditions, the power generated will be around 100W, but practically, the power generated in this scenario is approximately 94.5W. From scenario-2 it is clear that despite the input variations, the system showed fast recovery, and the controller continued to track the power and mitigate the variations. Note that, the

switching action usually creates a rough drag, and when disturbances are observed, the curve goes unevenly. Hence, the proposed ITSMC was able to eliminate the switching action, though some immediate disturbances were noted in scenario-3.

V. CONCLUSION

This paper presented an integral terminal sliding mode control scheme for a grid-connected PV array under various operating conditions. The design was based on a new sliding surface and aimed at maximizing power extraction while mitigating the effects of disturbances caused by fluctuations in irradiance and oscillations in the bulk voltage. The reference for maximum power point tracking was generated by the easily implemented perturb and observe algorithm. An IGBT switch was used in the design instead of BJT or MOSFET for better power production. The obtained results clearly showed that the proposed ITSMC was able to achieve finite time convergence of the error to zero. Excellent tracking performance as well as effective mitigation of voltage sags were also noted. Further, the proposed ITSMC was able to eliminate the power chattering while searching for MPP.

REFERENCES

[1] J. M. Carrasco, L. G. Franquelo, J. T. Bialasiewicz, E. Galvan, R. C. P. Guisado, M. A. M. Prats, J. I. Leon, N. Moreno-Alfonso, "Power-electronic systems for the grid integration of renewable energy sources: A survey*," IEEE Trans. Ind. Electron*., vol. 53, no. 4, pp. 1002– 1016, Aug. 2006.

[2] A. L. Fahrenbruch, R. H. Bube, Fundamentals of Solar Cells. San Francisco, CA: Academic, 1983

[3] M. A. S. Masoum, H. Dehbonei, E. F. Fuchs, "Theoretical and experimental analyses of photovoltaic systems with voltage and current-based maximum power-point tracking," *IEEE Trans. Energy Convers*., vol. 17, no. 4, pp. 514–522, Dec. 2002.

[4] R.N. Tripathi, T.Hanamoto, "FRIT based optimized PI tuning for DC link voltage control of grid connected solar PV systems," *Proc. of IEEE Conf. on Indus. Electro*., pp. 1567-1572, Nov. 2015.

[5] F.J. Lin, K-C. Lu, T-H. Ke, B-H. Yang, Y-R. Chang "Reactive power control of three-phase grid-connected PV system during grid faults using Takagi–Sugeno–Kang probabilistic Fuzzy Neural Network Control" *IEEE Trans. Ind. Elec*., vol.62, no.9, pp.5516-5528, 2015.

[6] E.C. Chang, T.J. Liang,J.F. Chen,F.J. Chang, "Real-time implementation of grey fuzzy terminal sliding mode control for PWM DC‐AC converters," *IET Pow. Electr.*, vol.1, no.2, pp.235‐244, 2008.

[7] H.M. Hasanien, "An adaptive control strategy for low voltage ride through capability enhancement of grid-connected photovoltaic power plants," *IEEE Trans. on Pow. Sys*., vol.31, no.4, pp. 3230-3237, 2016.

[8] A. Kulkarni,V. John" Mitigation of lower order harmonics in a grid- connected single phase PV inverter" *IEEE trans. on Power Electronics*, vol. 28, no. 11, pp. 5024-5037, Nov. 2013.

[9] V. Utkin, J. Guldner, J. Shi, Sliding Mode Control in Electro Mechanical Systems, CRC Press, 2009.

[10] M. J. Morshed, A. Fekih, "Integral terminal Sliding Mode Control to provide fault ride-through capability for a grid connected wind turbine driven DFIG," *Proc. of IEEE Int. Conference on Industrial Technology*, pp. 1059-1064, Mar. 2015.

[11] M. J. Morshed, A. Fekih, "A fault-tolerant control paradigm for microgrid-connected wind energy systems," *IEEE Systems Journal*, vol. PP, No. 99, pp. 1-13, 2016.

[12] G. Bartolini, L. Fridman, A. Pisano, E. Usai, *Modern Sliding Mode Control Theory,* Springer 2008.

[13] N. Femia, G. Petrone, G. Spagnuolo, and M. Vitelli, "Optimization of perturb and observe maximum power point tracking method," *IEEE Trans. Power Electron*., vol. 20, no. 4, pp. 963–973, Jul. 2005.

[14] E. Bianconi, J. Calvente, R. Giral, E. Mamarelis, G. Petrone, C.A. Ramos- Paja, G. Spagnuolo, andM. Vitelli, "Perturb and observe MPPT algorithm with a current controller based on the sliding mode," *Int. J. Electr. Power Energy Syst*., vol. 44, no. 1, pp. 346–356, 2013.

[15] E. Mamarelis, G. Petrone, and G. Spagnuolo, "Design of a sliding-mode controlled SEPIC for PV MPPT applications," *IEEE Trans. Ind. Electron*., vol. 61, no. 7, pp. 3387–3398, 2014.

[16] Y. Levron and D. Shmilovitz, "Maximum power point tracking employing sliding mode control," *IEEE Trans. Circuits Syst.* , vol. 60, no. 3, pp. 724–732, Mar. 2013.

[17] D. G. Montoya, C. A. Ramos-Paja, R. Giral "Improved Design of Sliding-Mode Controllers Based on the Requirements of MPPT Techniques" *IEEE transactions on Power Electronics*, vol. 31, no. 1, pp. 235-247, Jan. 2016.

[18] C. S. Chiu, "Derivative and integral terminal sliding mode control for a class of MIMO nonlinear systems," *Automatica*, vol. 48, no. 2, pp. 316-326, Feb. 2012.

[19] M. J. Morshed, A. Fekih, "A Comparison Study Between two Sliding Mode Based Controls for Voltage Sag Mitigation in Grid Connected Wind Turbines" *Proc. of IEEE Multi-Conference on Systems and Control*, pp. 21-23, Sydney, Australia, Sep. 2015.

[20] M. G. Villalva, J. R. Gazoli, E. R. Filho, "Comprehensive Approach to Modeling and Simulation of Photovoltaic Arrays" *IEEE transactions on power electronics*, vol. 24, no. 5, may 2009.

[21] H. S. Rauschenbach, *Solar Cell Array Design Handbook*. New York: Van Nostrand Reinhold, 1980.

[22] X. Liu X., L.A.C. Lopez, "An improved perturbation and observation maximum power point tracking algorithm for PV arrays,", *Proc. of IEEE Power Electronics Specialists Conf*., 2004.

[23] S. Cuk, "Basics of switched-mode power conversion: topologies, magnetics, and control," *Advances in Switched-Mode Power Conversion*, vol. 2, pp. 279-310, Irvine: Teslaco, 1981.

[24] H-J. Choe, Y-C. Chung, C-H. Sung, J-J. Yun, B. Kang, "Passive Snubber for Reducing Switching-Power Losses of an IGBT in a DC–DC Boost Converter" *IEEE transactions on power electronics*, vol. 29, no. 12, December 2014.

[25] T. Esram and P. L. Chapman, "Comparison of photovoltaic array maximum power point tracking techniques," *IEEE Trans. Energy Convers*., vol. 22, no. 2, pp. 439–449, Jun. 2007.

[26] M. Salem, Y. Atia" Control scheme towards enhancing power quality and operational efficiency of single-phase two-stage grid-connected photovoltaic systems" *J. of Electrical Systems and Information Technology*, vol.2, no. 3, pp.314-327, May 2015.

[27] C. Chiu., C Shen., "Finite-time control of DC-DC buck converters via integral terminal sliding modes," *International Journal of Electronics,* vol. 99, no. 5, pp .643-655, 2012.